

Dictyostelium discoideum CenB Is a Bona Fide Centrin Essential for Nuclear Architecture and Centrosome Stability[∇]

Sebastian Mana-Capelli,¹ Ralph Gräf,² and Denis A. Larochelle^{1*}

Department of Biology, Clark University, 950 Main Street, Worcester, Massachusetts 01610,¹ and Institut für Biochemie und Biologie, ZELLBIOLOGIE, Universität Potsdam, Karl-Liebknecht-Strasse 24-25, Haus 26, 14476 Potsdam-Golm, Germany²

Received 17 January 2009/Accepted 13 May 2009

Centrins are a family of proteins within the calcium-binding EF-hand superfamily. In addition to their archetypical role at the microtubule organizing center (MTOC), centrins have acquired multiple functionalities throughout the course of evolution. For example, centrins have been linked to different nuclear activities, including mRNA export and DNA repair. *Dictyostelium discoideum* centrin B is a divergent member of the centrin family. At the amino acid level, DdCenB shows 51% identity with its closest relative and only paralog, DdCenA. Phylogenetic analysis revealed that DdCenB and DdCenA form a well-supported monophyletic and divergent group within the centrin family of proteins. Interestingly, fluorescently tagged versions of DdCenB were not found at the centrosome (in whole cells or in isolated centrosomes). Instead, DdCenB localized to the nuclei of interphase cells. This localization disappeared as the cells entered mitosis, although *Dictyostelium* cells undergo a closed mitosis in which the nuclear envelope (NE) does not break down. DdCenB knockout cells exhibited aberrant nuclear architecture, characterized by enlarged and deformed nuclei and loss of proper centrosome-nucleus anchoring (observed as NE protrusions). At the centrosome, loss of DdCenB resulted in defects in the organization and morphology of the MTOC and supernumerary centrosomes and centrosome-related bodies. The multiple defects that the loss of DdCenB generated at the centrosome can be explained by its atypical division cycle, transitioning into the NE as it divides at mitosis. On the basis of these findings, we propose that DdCenB is required at interphase to maintain proper nuclear architecture, and before delocalizing from the nucleus, DdCenB is part of the centrosome duplication machinery.

Centrins (also known as caltractins) are small calcium-binding proteins of the EF-hand superfamily and are thought to have diversified by gene duplication (37). The first centrin was discovered in the unicellular green algae *Tetraselmis striata* more than 20 years ago (45). Since then, members of this family of proteins have been found in groups as diverse as yeasts, insects, plants, and humans, making these proteins essentially ubiquitous among eukaryotic cells (55). Furthermore, centrins have been included within the 347 “eukaryotic signature proteins” that are thought to be indispensable for the eukaryotic cell and share no similarities with prokaryotic proteins (21). Many lower eukaryotes have a single centrin gene (e.g., *Saccharomyces cerevisiae* and *Chlamydomonas reinhardtii*); however, up to three or four centrin paralogs have been found in higher eukaryotes (e.g., *Xenopus laevis*, *Mus musculus*, and *Homo sapiens*). Centrins have a high level of structural resemblance to calmodulin, exhibiting the characteristic two globular domains interconnected by a linker loop. Each globular domain in turn contains two helix-loop-helix motifs that, in calmodulins, bind calcium ions. However, in many centrins these motifs are slightly modified, and not all four of them have affinity for calcium in the normal range associated with signal transduction (33).

Throughout the course of evolution, centrins have acquired multiple functionalities in addition to the archetypical role at the microtubule organizing center (MTOC). For example, the

centrin of the flagellated green algae *C. reinhardtii* (CrCen) localizes to the basal bodies, to the fibers that interconnect the basal bodies and the nucleus, and to the axoneme. CrCen is required for normal basal body replication, segregation, and maturation (26). In addition, it plays an active role in the contraction of MTOC-related fibers (47, 57) and regulates the activity of the inner dynein arm in a calcium-regulated fashion (30).

In the budding yeast *Saccharomyces cerevisiae*, centrin (ScCDC31) localizes primarily to a specialized region of the nuclear envelope (NE) called the half bridge (49), which is in close proximity to the MTOC (known as the spindle pole body [SPB]). Conditional mutants of ScCDC31 show cell cycle arrest and failure to duplicate the SPB (23, 49). CDC31 also binds the NEF2 complex and is required for efficient nucleotide excision repair. CDC31 mutants unable to bind to the complex showed an increased sensitivity to UV (1). In addition, CDC31 is involved in mRNA export through its interaction with SAC3 at the nuclear pore (11). Mammalian cells typically have four centrin paralogs; however, human cells express only three (HsCen1 to -3) and the fourth is a pseudogene (gene ID, 729338) (9, 13, 31, 36). All human centrins show partial localization at the centrioles, in a tissue-specific fashion (HsCen1) or ubiquitously (HsCen2 and -3) (29, 56). Knockdown of HsCen2 inhibits centriole duplication and induces cell division arrest in HeLa cells (46). Additionally, HsCen2 was shown to play a role similar to that of CDC31 in stimulating nucleotide excision repair by binding to xeroderma pigmentosum group C protein (38).

The social amoeba *Dictyostelium discoideum* has emerged as a powerful model organism, in part because it is haploid, it is

* Corresponding author. Mailing address: Department of Biology, Clark University, 950 Main Street, Worcester, MA 01610. Phone: (508) 793-7631. Fax: (508) 793-7174. E-mail: dlarochelle@clarku.edu.

[∇] Published ahead of print on 22 May 2009.

easy to propagate, and its genome has been recently completed (4, 8, 25). *D. discoideum* cells undergo a closed mitosis during which the NE remains intact. They also have multiple modes of cytokinesis (53), making them a very useful model for studying the cell division machinery. These cells lack basal bodies and have acentriolar centrosomes that are similar in their trilaminar core structure to yeast SPBs (17). However, *D. discoideum* interphase centrosomes are not embedded in the NE but are attached to it, and they are surrounded by a centrosomal corona analogous to the pericentriolar material of animal cell centrosomes (4). Centrosomal duplication in *D. discoideum* involves extensive structural changes and is synchronized with mitosis. It begins at early prophase, by increasing its size to about twice that of an interphase centrosome. At the prophase-prometaphase transition, the corona and the fibrous link to the nucleus are disassembled. This is followed by the insertion of the core into the NE. By metaphase, the two outer layers have come apart and migrated to opposite ends of the cell nucleus, where they organize the spindle. The anaphase-telophase transition marks the beginning of centrosomal maturation. The outer layers fold back into themselves, inducing the formation of a middle layer and a corona, and returning to the size of an interphase centrosome. Finally, the two maturing centrosomes transition out of the NE at the end of mitosis and reform the fibrous link that connects them to the NE (17, 52). It has recently been shown that the *D. discoideum* Sun1 protein is a key component of the fibrous link that bridges and anchors the centrosome to the cell nucleus (58). DdSun1 predominantly localizes to the nuclear membrane and links chromatin to other components of the fibrous link. Truncation or knock-down of DdSun1 promotes separation of the inner and outer NE membranes, inducing aberrant nuclear morphology and loss of the nucleus-centrosome connection (observed as protrusions of the outer NE membrane). Additionally, cells develop supernumerary centrosomes and aberrant spindles, leading to poor chromosome segregation. All this suggests that the centrosome-nucleus link is of extreme importance in maintaining the genetic stability of the cell.

D. discoideum has two known centrin proteins, DdCenA (originally named DdCrp) and DdCenB. The initial characterization of DdCenA describes a very divergent centrin that localizes to the centrosomal corona and to the nucleus (5). The second centrin protein, known as DdCenB, was originally identified as a putative member of the centrin family based on sequence similarity by the *Dictyostelium* Genome Consortium and remained uncharacterized until now. In this work, we report the initial characterization of DdCenB, including molecular cloning, sequence analysis, cellular localization, and analysis of functional roles.

MATERIALS AND METHODS

D. discoideum strain AX3 was cultured in HL5 media (yeast extract, 10 g/liter; thiotone E peptone, 15 g/liter; proteose peptone, 15 g/liter; glucose, 20 g/liter; Na₂HPO₄, 0.7 g/liter; KH₂PO₄, 2.4 g/liter; pH 6.5) at 18°C and with shaking (200 rpm). In all cases the media was supplemented with penicillin-streptomycin (100 U/100 µg/ml; GIBCO). Cell lines transfected with pTX-mRFPmars, pTX-FLAG, and pTX-GFP (32) were selected with gentamicin (10 µg/ml; GIBCO).

Molecular cloning and protein expression. Total RNA was extracted from *Dictyostelium* cells using TRIzol (Invitrogen). Briefly, 1 × 10⁸ cells were collected, lysed with 1 ml of TRIzol, and centrifuged at 12,000 × g for 10 min. To the supernatant, 200 µl of chloroform was added, and the solution was centri-

fuged again at 12,000 × g. The aqueous layer was transferred to a clean tube, and the RNA was precipitated with isopropanol and resuspended in water. Total RNA was quantified, and 200 ng was used to generate cDNA with an Accuscript high-fidelity reverse transcriptase PCR system (Stratagene). Full-length DdCenB was amplified from the cDNA using the primers 5'-GGGATCCGTAAAAACA AATACAAATAAATTAACAGAC-3' and 5'-GCTCGAGTTATAAAACCTT TTTAGTTGTCATTAATG-3' and cloned using a Qiagen PCR cloning kit (Qiagen). Sequences were confirmed by automated sequencing. For protein expression experiments, the coding sequence of DdCenB was subcloned in pTX-mRFP, pTX-FLAG, and pTX-GFP and transfected in *D. discoideum* strain AX3 using a Gene Pulser electroporator with a pulse controller (Bio-Rad). These constructs use the constitutive A15 promoter. FLAG-DdCenB was detected in Western blots with anti-FLAG M2 (Sigma).

Generation of the knockout mutant. DdCenB knockout strains were generated using a modified restriction enzyme-mediated integration (REMI) plasmid rescued from an insertion in the DdCenB locus. Briefly, a plasmid that had integrated within the first 100 bp of the DdCenB coding sequence was obtained from a genome-wide mutagenesis screen that was undertaken several years ago as a resource for the *Dictyostelium* community (7). Unlike most cases, where a simple linearization of the plasmid and subsequent transfection allow for the recreation of the insertion, the desired mutants could not be generated after repeated attempts (possibly due to the high level of A-T repeats in the DNA flanking the DdCenB locus). We therefore deleted the flanking sequences outside of the coding region by inward PCR amplification using the primers described above at the 5' and 3' ends of DdCenB (see Fig. 5A). The purified amplicon was then used for homologous recombination to disrupt the DdCenB locus, yielding several clonal cell lines. These cell lines were screened by PCR using a primer on the vector and a second one outside of the recombination site (see Fig. 5).

Cell fractionation. In order to visualize red fluorescent protein (RFP)-DdCenB in a centrosome-nuclear enriched fraction, cells (5 × 10⁹) expressing the fusion protein were centrifuged at 800 × g for 10 min and washed three times with phosphate-buffered saline (PBS) buffer. The pellet was resuspended in 1 ml of lysis buffer (100 mM Na-PIPES [piperazine-N,N'-bis(2-ethanesulfonic acid)], pH 6.9, 10% sucrose, 0.25% Triton X-100, 5 µg/ml leupeptin, 1 mM phenylmethylsulfonyl fluoride, 1.4 µg/ml pepstatin), vortexed for 1 min, and passed through a Nuclepore filter (Whatman) with a pore size of 5 µm. The filtrate was immediately centrifuged at 200 × g, and the pellet was discarded. The resulting supernatant was centrifuged at 600 × g, and this pellet was resuspended in 200 µl of lysis buffer. Half of the volume was then centrifuged onto a coverslip at 2,250 × g for 10 min to allow adhesion of the organelles to the glass. Immunofluorescence was performed on the cellular fraction as described below. This procedure was modified from the method in reference 14. Nuclear and soluble fractions were also obtained from cells expressing green fluorescent protein (GFP)-DdCenB and GFP-Sun1. Nuclear fractions were obtained by centrifugation at 1,000 × g. The remaining supernatants were further centrifuged at 20,000 × g, and the resulting supernatants were considered the soluble fractions. Protein concentration was standardized by Bradford assay, and their relative abundance levels were analyzed by Western blotting using anti-GFP antibody (Sigma).

Microscopy. *D. discoideum* whole cells and cellular fractions were fixed for 5 min in cold methanol. When indicated, cells were incubated in DAPI (4',6-diamidino-2-phenylindole) solution (100 ng/ml of DAPI in PBS) for 10 min followed by three washes with PBS to remove unincorporated DAPI. Immunofluorescence was performed as indicated on whole cells, and the centrosome-nuclear enriched fraction was incubated with anti-DdCP224 (15), anti-β-tubulin (Developmental Studies Hybridoma Bank at the University of Iowa), anti-γ-tubulin (10), anti-DdSp97 (3), anti-DdSun1 (I. Schultz, O. Bauman, C. Zoglmeier, M. Samereier, and R. Gräf, unpublished data), or anti-FLAG M2 (Sigma) for 1 h, followed by three washes and a 1-h incubation with anti-mouse Alexa 568, anti-mouse Alexa 488, or anti-rabbit Alexa 488. DNA was stained with DAPI. Confocal images were captured with Metamorph software (Universal Imaging Corp.) and processed with ImageJ (41).

Phylogenetic analysis. The sequence data set included three families of the EF-hand superfamily of proteins: centrans, calmodulins, and spasmins (all sequences were downloaded from GenBank). The alignment was performed with Clustal X as implemented in BioEdit 7.0.5.3 (20) and improved by hand. The short sequences that extended beyond the globular domains were disregarded for the phylogenetic analysis due to the low level of homology. Phylogenetic relationships were estimated by the maximum parsimony method using PAUP* v. 4.0b. Support values were generated by bootstrap and Bayesian analyses. The parsimony bootstrap analysis was performed using 10,000 replicates with 10 random sequence additions per replicate. The consensus phylogram was generated using an 80% consensus rule. The Bayesian analysis was run in MrBayes

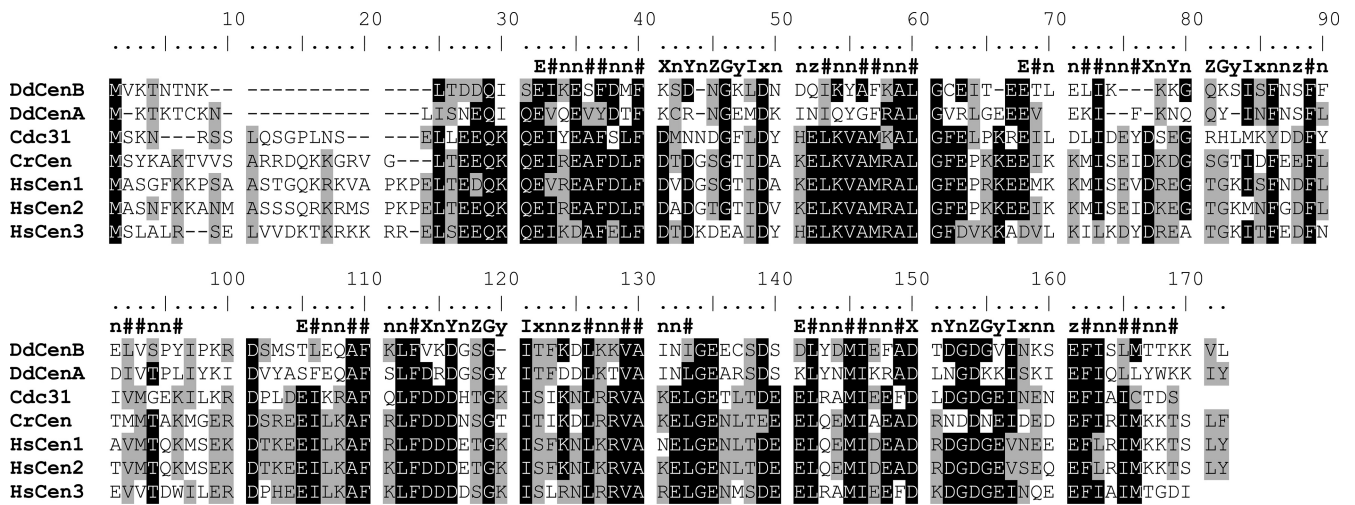


FIG. 1. Sequence alignment of DdCenB with other members of the centrin family. The four canonical EF-hand consensus motifs are shown at the top of the alignment. X, Y, Z, x, and z: residues containing oxygen in the side chains that provide five of the six coordination points for the interaction with calcium. y: residue with a carbonyl oxygen that provides the sixth coordination point. I, L, or V. #: hydrophobic residues. n: any residue. Identities shared by at least five of the sequences are shaded in black. Similar amino acids shared by at least four of the sequences are shaded in gray. The alignment was performed with BioEdit 7.0.5.3.

3.1.2 (43) using eight chains for 1,100,000 generations, sampling every 1,000 trees and with a burn-in of 100 trees.

RESULTS

DdCenB is part of a divergent group of centrins. Amplification of the full-length coding sequence of DdCenB yielded an amplicon of 450 nucleotides, which was an exact match with the predicted sequence (gene ID, 66815669). The DdCenB gene encodes a 150-amino-acid protein, with a predicted size of 16.9 kDa and a pI of 4.67, which is in the range of known centrins (48). Figure 1 shows the alignment of DdCenB with its paralog DdCenA and the centrin homologs in *S. cerevisiae*, *C. reinhardtii*, and *H. sapiens*. The canonical EF-hand conserved motifs are shown on top of the alignment, including the six residues (X, Y, Z, x, y, z) that can coordinate calcium (37). The level of homology of DdCenB to the other centrin sequences reveals 51% identity and 70% similarity to DdCenA and only between 37 and 38% identity and 65 to 66% similarity to human centrins. The unusually low level of conservation of DdCenB is striking. As an example of a comparable unicellular eukaryote, the yeast centrin ScCDC31 reaches 58 to 61% identity and 73 to 80% similarity to human centrins. However, the level of DdCenB homology increases at the EF-hand subdomains, showing 50% identity and 82% similarity to the consensus sequence. The main structural feature that distinguishes centrins from calmodulins is a longer N-terminal extension (before the beginning of the first EF-hand). The DdCenB N-terminal extension is 15 amino acids long, only one amino acid shorter than its paralog DdCenA, which places DdCenB within the centrin family of proteins. The C terminus of DdCenB contains the positively charged duplet (KK) that is common to animal centrins 1 and 2 (represented here by HsCen1 and HsCen2) and some lower eukaryote centrins, such as CrCen. However, in those centrins, the duplet is part of a protein kinase A phosphorylation site (consensus sequence KKXS-X) that is incomplete in DdCenB, since the serine is

missing. In addition, the DdCenB KK motif is not entirely part of the EF-hand motif but is displaced toward the C-terminal end of the protein. This is common in DdCenA, which may imply an early mutation prior to the duplication event that led to the two *D. discoideum* centrins. This end of DdCenB also shows the three-amino-acid extension (after the fourth EF-hand) characteristic of centrins 1 and 2 and CrCen; however, it lacks the terminal aromatic residue.

The phylogenetic relationships between DdCenB and other members of the centrin family, as well as members of the calmodulin and spasmin families, are shown in Fig. 2. The different clades show sequence relationships that were resolved in at least 80% of the trees generated by bootstrapping. Sequences with low levels of resolved relationships were grouped together and are shown with no shading at the top of the alignment. The fact that all unresolved nodes correspond to centrin sequences reflects that the degree of divergence of centrins is higher than that of calmodulins. The phylogram shows that DdCenB and DdCenA do not cluster with members of the centrin 3 group (Fig. 2, group II) or with centrins 1 and 2 (group IV) but constitute a very divergent and monophyletic group (group I). This branch is very well supported by bootstrap (99%) and Bayesian (1.0) analyses. The strength of the support is actually higher than that for the calmodulin branch (group III). Although our emphasis has been on DdCenB, we believe this phylogram is useful for examining phylogenetic relationships between other centrins. For example, the group II clade encompasses animal centrins 3 and a number of lower eukaryote homologs (including ScCDC31), suggesting a common ancestor for these centrins. Other resolved clades are the plant centrins (group V) and the spasmins (group VI). The residue change bar shows the level of divergence and can be used to compare divergence within a clade. It is remarkable that the divergence between the two *D. discoideum* centrins is greater than that between members of any other clade, including the spasmins.

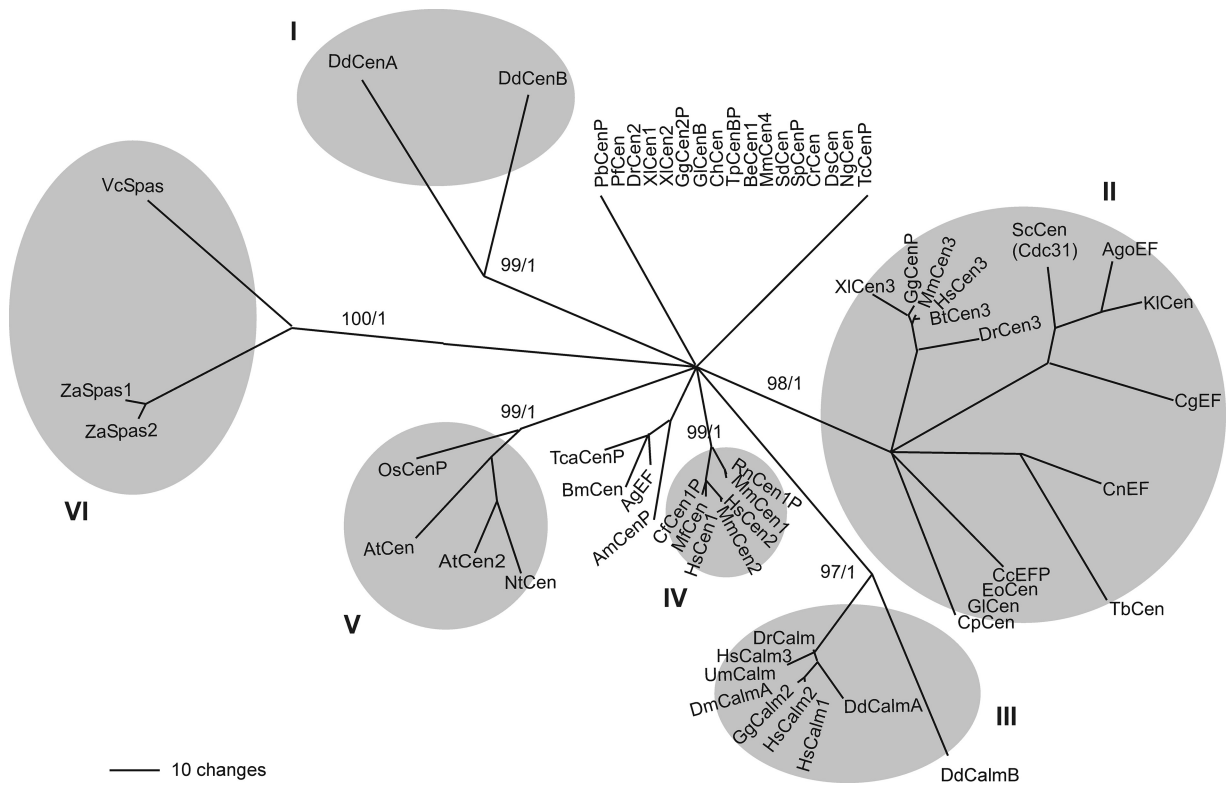


FIG. 2. Phylogenetic analysis shows that DdCenB, together with DdCenA, constitutes a divergent clade within the EF-hand superfamily of proteins (I). The main clades are shaded, and the bootstrap (top) and Bayesian support values (bottom) are shown for each one of them. Resolved sequences in this phylogram were present in at least 80% of the trees generated by Bootstrap, otherwise they are shown as unresolved. Nonconserved sequence flanking the four EF-hand domains at the N and C termini of all proteins were disregarded in this analysis. Cen, centrin; Calm, calmodulin; Spas, spasmin; EF, EF-hand-containing protein. Putative proteins were labeled with a “P” at the end of the name. GI, gene identification as annotated at NCBI (<http://www.ncbi.nlm.nih.gov/sites/entrez?db=Protein&itool=toolbar>). The phylogenetic relationships were estimated by the maximum parsimony analysis using PAUP* v. 4.0b. Bayesian analysis was performed with MrBayes 3.1.2 using eight chains for 1,100,000 generations, sampling every one thousand trees and with a burn-in of 100 trees. AgEF, *Anopheles gambiae* STR.PEST (GI: 116117847); AgoEF, *Ashbya gossypii* (GI: 45184714); AmCenP, *Apis mellifera* (GI: 66529823); AtCen2, *Arabidopsis thaliana* (GI: 15229732); AtCen, *Arabidopsis thaliana* (GI: 2270650); BeCen1, *Blastocladiella emersonii* (GI: 70931046); BmCen, *Bombyx mori* (GI: 87248293); BtCen3, *Bos taurus* (GI: 111307090); CcEFP, *Coprinospis cinerea okayama* 7#130 (GI: 116509538); CfCen1P, *Canis lupus familiaris* (GI: 57089853); CgEF, *Candida glabrata* (GI: 50292355); ChCen, *Cryptosporidium hominis* TU502 (GI: 54658657); CnEF, *Cryptococcus neoformans* var. *neoformans* JEC21 (GI: 58270616); CpCen, *Cryptosporidium parvum* (GI: 46227249); CrCen, *Chlamydomonas reinhardtii* (GI: 159482892); DdCalmA, *Dictyostelium discoideum* AX4 (GI: 66815357); DdCalmB, *Dictyostelium discoideum* AX4 (GI: 66825411); DdCenA, *Dictyostelium discoideum* (GI: 66806051); DdCenB, *Dictyostelium discoideum* (GI: 66815669); DmCalmA, *Drosophila melanogaster* (GI: 17647231); DrCalm, *Danio rerio* (GI: 41054633); DrCen2, *Danio rerio* (GI: 189540405); DrCen3, *Danio rerio* (GI: 66472718); DsCen, *Dunaliella salina* (GI: 1705641); EoCen, *Euplotes octocarinatus* (GI: 75029523); GgCalm2, *Gallus gallus* (GI: 45384366); GgCen2P, *Gallus gallus* (GI: 50745880); GgCenP, *Gallus gallus* (GI: 118104383); GlCen, *Giardia lamblia* ATCC 50803 (GI: 159110457); GlCenB, *Giardia lamblia* ATCC 50803 (GI: 159114706); HsCalm1, *Homo sapiens* (GI: 5901912); HsCalm2, *Homo sapiens* (GI: 13623675); HsCalm3, *Homo sapiens* (GI: 13477325); HsCen1, *Homo sapiens* (GI: 4757974); HsCen2, *Homo sapiens* (GI: 4757902); HsCen3, *Homo sapiens* (GI: 46397403); KlCen, *Kluyveromyces lactis* (GI: 50305339); MfCen, *Macaca fascicularis* (GI: 67971808); MmCen1, *Mus musculus* (GI: 76253942); MmCen2, *Mus musculus* (GI: 10257421); MmCen3, *Mus musculus* (GI: 6680922); MmCen4, *Mus musculus* (GI: 22003866); NgCen, *Naegleria gruberi* (GI: 1705642); NiCen, *Nicotiana tabacum* (GI: 6358509); OsCenP, *Oryza sativa* (Japonica cultivar-group) (GI: 78708509); PbCenP, *Plasmodium berghei* (GI: 56499292); PfCen, *Plasmodium falciparum* 3D7 (GI: 124505775); RnCen1P, *Rattus norvegicus* (GI: 34877910); ScCen (Cdc31), *Saccharomyces cerevisiae* (GI: 6324831); SdCen, *Scherffelia dubia* (GI: 21209); SpCenP, *Strongylocentrotus purpuratus* (GI: 115898527); TbCen, *Trypanosoma brucei* TREU927 (GI: 72387904); TcaCenP, *Tribolium castaneum* (GI: 91081379); TcCenP, *Trypanosoma cruzi* (GI: 70886637); TpCenBP, *Theileria parva* strain Muguga (GI: 71027987); UmCalm, *Ustilago maydis* 521 (GI: 46099694); VcSpas, *Vorticella convallaria* (GI: 4100824); XlCen1, *Xenopus laevis* (GI: 1017791); XlCen2, *Xenopus laevis* (GI: 32766515); XlCen3, *Xenopus laevis* (GI: 11119117); ZaSpas1, *Zoothamnium arbuscula* (GI: 26453345); ZaSpas2, *Zoothamnium arbuscula* (GI: 26453347).

DdCenB subcellular localization. In order to study the subcellular localization of DdCenB, the full-length coding sequence was fused to RFP, FLAG, and GFP (independently) and expressed in *D. discoideum* cells. Cells were fixed with chilled methanol, stained with DAPI, and observed by wide-field epifluorescence microscopy (Fig. 3A to C). Surprisingly, both fluorescently tagged versions of DdCenB predominantly localized to the nuclei of interphase cells (Fig. 3A and B). In

addition, FLAG-DdCenB did not colocalize with the centrosome marker DdCP224 (16) at this level of resolution (Fig. 3C, inset). To further characterize the DdCenB subcellular localization, and in particular to determine if this protein was at least partially localizing to the centrosome, we observed cells and partially purified centrosomes by confocal microscopy (Fig. 3E and F). Observations of RFP-DdCenB at high magnification, and without out-of-focus fluorescence, showed that

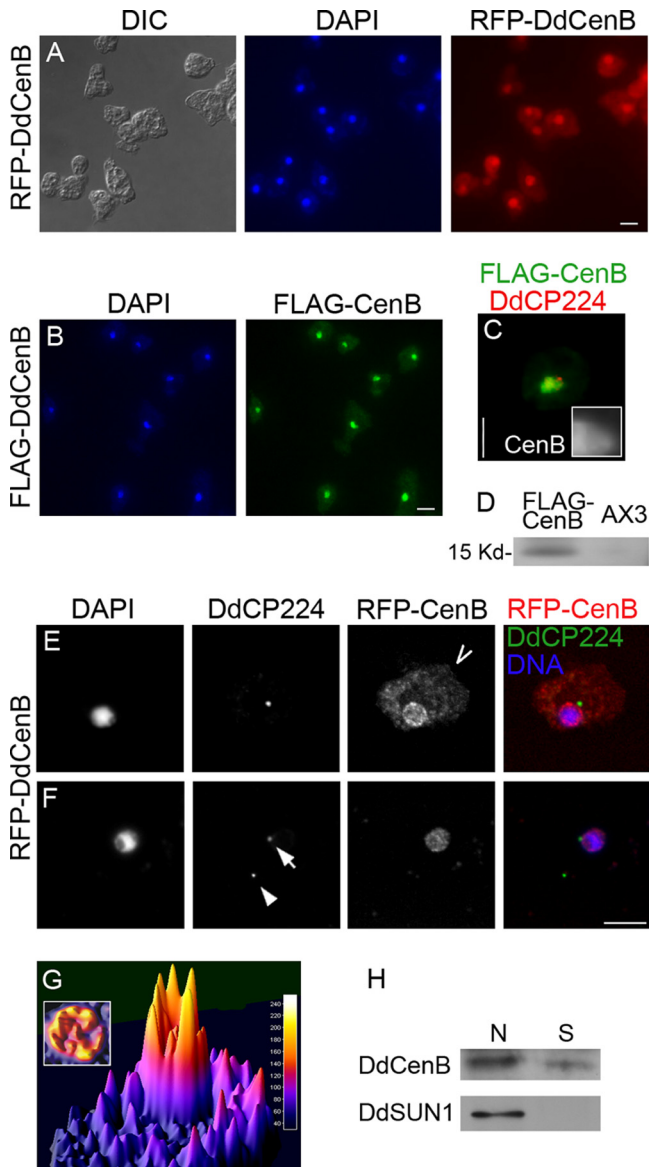


FIG. 3. DdCenB localizes to the nucleus but not to the centrosome. Epifluorescence images show cells expressing RFP-DdCenB (A) and FLAG-DdCenB (B). Additionally, cells expressing FLAG-DdCenB were also costained with anti-DdCP224 (C). The inset shows the centrosome region at 3 \times magnification. (D) Immunoblot of total cell extracts probed with anti-FLAG antibodies. RFP-DdCenB cells (E) and a purified centrosome/nucleus fraction (F) were also observed by confocal microscopy. Images are brightest point projection (E) and a single optical section at the focal plane of the centrosome (F). Cells were fixed with chilled methanol, labeled with antibodies (as indicated), and stained with DAPI. Centrosomes were isolated by differential centrifugation and stained identically to whole cells. The arrow points to a nucleus-attached centrosome and the arrowhead to a “free” centrosome. (G) Three-dimensional plot of fluorescence intensity of a single RFP-DdCenB-expressing cell (taken from panel E; the vantage point is marked with an open arrow). The inset shows the nuclear area viewed from above. (H) Cell fractionation of GFP-DdCenB-expressing cells. GFP-DdSun1 (a NE protein) was used as a control. N, nuclear; S, soluble. Secondary antibodies: anti-mouse Alexa 488 (panels E and F) and anti-rabbit Alexa 568 (panel C). All images are shown at the same magnification. Bars, 5 μ m. DIC, differential interference contrast.

most of the nuclear localization of RFP-DdCenB was confined to the NE, where it also formed foci of intense fluorescence (Fig. 3E). The position of these “hot spots” had no apparent relationship with the position of the centrosome (visualized with DdCP224), where no RFP-DdCenB was observed. The partially purified centrosome fraction obtained from cellular extracts was primarily composed of “free” and nuclei-attached centrosomes (which was particularly useful to confirm that the RFP-DdCenB was not photobleached during fractionation). Centrosomes were adhered to a glass slide by centrifugation and immunostained with antibodies against the centrosomal protein DdCP224. As seen in Fig. 3F, RFP-DdCenB did not localize to the nucleus-attached centrosome or the “free” centrosome (visualized by DdCP224 staining). The subcellular localization of DdCenB was further analyzed by surface plot profiling and cell fractionation. Figure 3G shows a three-dimensional representation of the fluorescence intensity of RFP-DdCenB observed in Fig. 3E. The vantage point was selected for better illustration of the difference in RFP-DdCenB abundance levels between the nucleus and the cytoplasm. Although a considerable amount of RFP-DdCenB was cytoplasmic, most of the centrin protein localized to the nuclear periphery and, to a lesser extent, to the nucleoplasm. This is highlighted in the inset, where the nuclear area is shown from the top. Cell fractionation was performed using GFP-DdCenB- and GFP-Sun1-expressing cells. GFP-Sun1 was used as a control for the fractionation, since it does not localize to the cytoplasm (58). Immunoblots of the fractions, standardized by protein content, are shown in Fig. 3H. These results are consistent with previous observations that most of the centrin protein localizes to the nucleus.

We were also intrigued to know if the nuclear localization of DdCenB changes during the cell cycle (recall that *D. discoideum* cells undergo a closed mitosis). Cells expressing RFP-DdCenB were immunostained with anti-tubulin antibody to visualize the spindle, and the nuclei were stained with DAPI. In contrast to interphase cells (Fig. 4A), DdCenB was no longer visible in the nuclei of cells with condensed DNA and early spindles (Fig. 4B, early mitosis). RFP-DdCenB was also absent from the nuclei of cells undergoing later stages of mitosis (Fig. 4C) and cytokinesis (Fig. 4D and E), indicating that this protein relocalizes to the nucleus after the completion of cytokinesis. Since *D. discoideum* cells have the ability to undergo cytokinesis through alternative mechanisms, we were also interested in determining if the localization of DdCenB would change in cells undergoing traction-mediated cytofission. This type of primitive cytokinesis is not under the regulation of mitotic kinases and is uncoupled from the cell cycle (53). In *D. discoideum* cells, a small subpopulation of the axenic culture usually fails to undergo the more common types of cell cycle-coupled cytokinesis. Those cells become multinucleated, and some of them will eventually try to divide by cytofission, which is easily detected by a simple DAPI staining, since there is no DNA condensation. Figure 4F shows a trinucleated cell undergoing traction-mediated cytofission (notice that the nuclear material is not condensed). In this cell, DdCenB remained associated with the nuclei throughout cell division. This is in contrast to what occurs in mitotic nuclei and suggests that the loss of DdCenB from mitotic nuclei may be

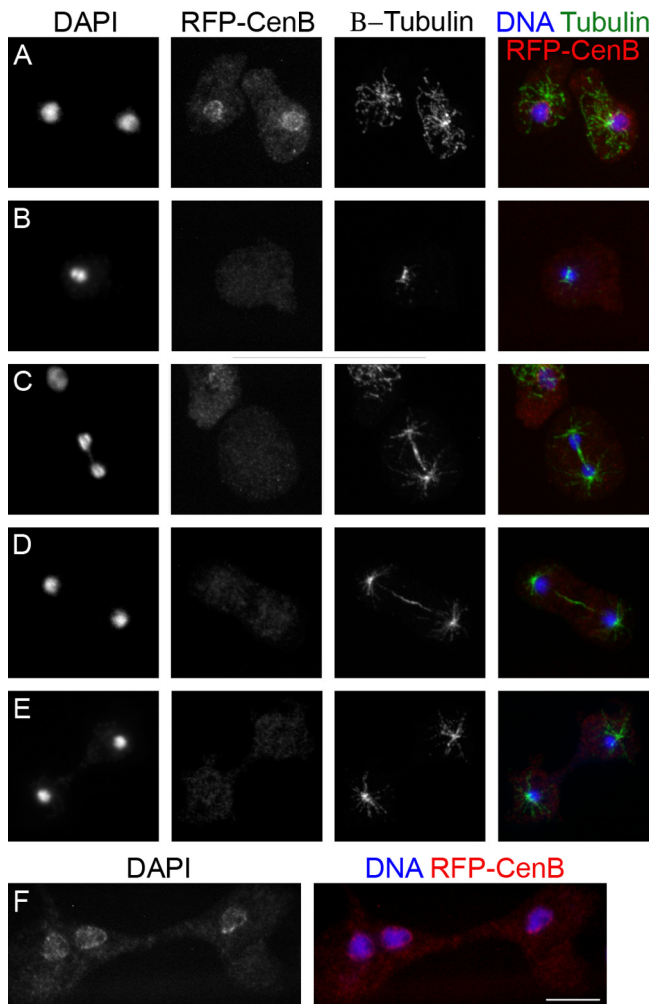


FIG. 4. The nuclear localization of RFP-DdCenB is bound to the cell cycle. Confocal microscopy images show the loss of nuclear localization of RFP-DdCenB as cells enter mitosis and continue through to cytokinesis. A, interphase; B, early mitosis; C, late mitosis; D, early cytokinesis; E, late cytokinesis. RFP-DdCenB remains at the nuclei of cells undergoing traction-mediated cytofission (F). Images are collapsed frames from stacks of 11 slices of 0.2 μm each. Cells expressing RFP-DdCenB were fixed with chilled methanol, labeled with antibodies against β -tubulin (as indicated), and stained with DAPI. Secondary antibody: anti-mouse Alexa 488. Bar, 5 μm .

regulated by the cell cycle machinery. Alternative explanations are addressed later (see Discussion).

Lack of DdCenB induced nuclear and centrosome abnormalities. REMI has proven to be an efficient means of insertional mutagenesis in *Dictyostelium*. The integrating plasmid is typically recovered by digestion and circularization of DNA containing both the plasmid and flanking genomic DNA (gDNA) (19, 28). One such recovered plasmid, with an integration site in the first 100 bp of the DdCenB coding sequence, was obtained from a genome-wide REMI mutagenesis effort (7), was modified (see Materials and Methods), and was used to recreate the gene disruption by homologous recombination in AX3 cells. Mutant cell lines were isolated and integration was confirmed by PCR. Figure 5B shows the amplified PCR product using gDNA from one of the isolated cell lines, con-

firmed that the construct integrated at the correct site. PCRs assembled with control template DNA (wild-type gDNA and the original REMI plasmid) yielded no amplicons. For further characterization, cell lines containing confirmed disruptions of the DdCenB locus were washed in starvation buffer and allowed to develop on 0.45- μm HA filters (Millipore) in 3-cm plates. The formation of mature fruiting bodies containing viable spores indicated that DdCenB is not required for development and spore formation in *Dictyostelium*.

Concurrent with the phenotypic analysis of the knockout strains, we wished to confirm that any observed phenotypes were in fact due to the disruption of DdCenB. This was achieved by the expression of RFP-DdCenB in the knockout strain. We began by investigating if the lack of centrin B had any effect on actomyosin-based cytokinesis (also called cytokinesis A) (53). As described above, *Dictyostelium* cells can undergo different modes of cytokinesis; however, if grown under suspension conditions, they can only divide through cytokinesis A. A small fraction of wild-type cells do become binucleated after several days under such conditions; therefore, cells quantified as “multinucleated” contained three or more nuclei. After 4 days of growth in suspension, cells were fixed and stained with DAPI. Surprisingly, the frequency of multinucleated knockout cells grown at 18°C was triple that of AX3 or the rescued cell lines (Fig. 5C). Furthermore, this increase in multinucleation was exacerbated by thermal stress, where knockout cells grown at 25°C exhibited a rise in frequency of multinucleation to approximately 45% (representative multinucleated cells are shown in Fig. 5C, inset). In contrast, the frequency of multinucleation of AX3 and RFP-DdCenB rescued cells remained low at 18°C, increasing only to 9% at 25°C. Virtually no multinucleated cells were observed in any cultures when grown in stationary plates (data not shown).

At the cellular level, disruption of DdCenB induced defects at the centrosome, the nucleus, and the cell division machinery. The tendency of DdCenB knockout cells to be multinucleated led us to examine the mitotic spindle by indirect immunofluorescence. Cells were costained with antibodies against β -tubulin and DdCP224 (here DdCP224 is used as a centrosome marker, although it has also been shown to label plus ends of interdigitating microtubules of the mitotic spindle [42]). Figure 6A, panels I to III show early spindles with disorganized and unfocused microtubules, sometimes radiating outwards from sites other than the poles (Fig. 6A, panel I'). DdCP224 was no longer primarily observed at the mitotic poles in these spindles but rather was diffusely localized along the spindle microtubules (Fig. 6A, panel I'). Cells lacking DdCenB also showed late cytokinesis defects when grown on plates, characterized by long interconnections resembling cytoplasmic bridges between daughter cells (Fig. 6A, panel IV). However, microtubule staining revealed that these cellular connections contained microtubules, possibly remnants of spindle midzones that had not fully disassembled (Fig. 6A, panel V). Lack of DdCenB not only compromised the integrity of mitotic poles but also led to multiple defects in interphase centrosomes. Figure 6B, panel I shows a representative cell with poor microtubule nucleation (a cell with normal nucleation is shown at the left, as a control). Interestingly, cells with poor microtubule nucleation also had diffusely localized β -tubulin around the MTOC (Fig. 6B, inset in panel I). Examining DdCP224 revealed unorganized stain-

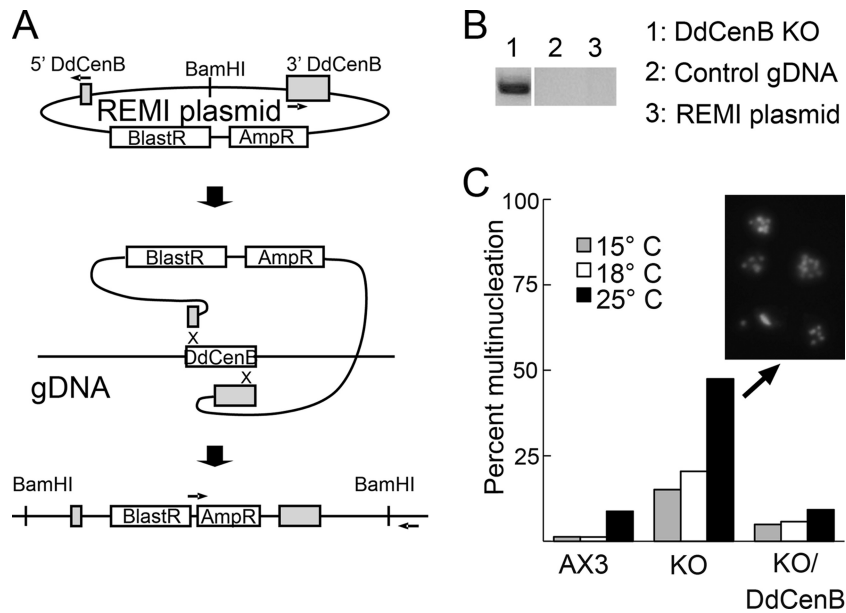


FIG. 5. Generation of the DdCenB knockout (KO) cell line and its impact on cytokinesis. (A) Schematic diagram of the creation of the DdCenB knockout construct by PCR and subsequent insertion by homologous recombination. (B) Diagnostic PCR confirming disruption of the DdCenB locus. (C) DdCenB knockout cells show a higher frequency of multinucleation than AX3 and the RFP-DdCenB rescued cell lines. Cells were grown at the described temperatures for 4 days at 200 rpm, fixed with chilled methanol, and stained with DAPI. Nuclei frequencies reflect cell numbers of at least 300 per data point.

ing rather than the typical ring-shaped corona that normally surrounds the centrosome core. Therefore, in some cases the loss of DdCenB seems to compromise the centrosome protein composition, leading to poor microtubule nucleation. Enlarged centrosomes with well-defined coronas were also detected by DdCP224 staining (Fig. 6B, insets in panels II and III). These centrosomes were usually associated with the nucleus and showed normal microtubule nucleating activity. Interestingly, cells with enlarged but well-defined centrosomes also had enlarged nuclei. It was not unusual to see some of these nuclei reaching three to four times the size of an average nucleus (Fig. 6B, panel III). The morphology of the enlarged nuclei was oftentimes compromised, becoming elongated or even “dumbbell” shaped (Fig. 6B, panel II).

Over 19% of the cells lacking DdCenB (19 out of 98 cells) also exhibited supernumerary MTOCs and centrosome-related bodies that stained with one or more centrosome markers (Fig. 6C). Centrosome structures were defined by the amount of microtubule nucleation and morphology at the level of fluorescence microscopy. Supernumerary centrosomes exhibited normal microtubule nucleation and were similar in shape and size to the nucleus-associated centrosome (Fig. 6C, panel I). However, the size of the centrosome-related bodies ranged from that of a nucleus-associated centrosome (Fig. 6C, panel I) to scattered foci of various sizes (Fig. 6C, panel II). A common characteristic shared by these centrosome-related bodies was their ability to localize β -tubulin but with very little or no nucleation of microtubules (Fig. 6C, insets in panels I and II). To further characterize the protein composition of the centrosome-related bodies, we decided to costain DdCenB knockout cells with antibodies against DdCP224 and other centrosome corona proteins. Figure 6C, panel III shows that in some cells, the γ -TuRC component DdSpc97 colocalized with DdCP224

regardless of the foci size. Although DdCP224 and DdSpc97 colocalized at these centrosome-related bodies, their staining patterns were not equivalent (Fig. 6C, insets in panel III), suggesting that these proteins localize independently. In Fig. 6C, panel IV, DdCP224 staining is faint at the MTOC but strong at the centrosome-related body. This contrasts with the localization of DdSpc97, which stained brightly at the nucleus-associated centrosome. It was not possible in this case to assess the microtubule nucleating activity of the bright DdCP224 “body” due to technical limitations, but in costaining experiments involving DdCP224 and β -tubulin, bright DdCP224 foci always showed limited microtubule nucleating activity (see insets in panel I of Fig. 6C). Similarly, costaining with DdCP224 and γ -tubulin revealed that both centrosome markers colocalize to some of the centrosome-related bodies (Fig. 6C, panel V), but γ -tubulin is absent in some others at this level of resolution (Fig. 6C, panel VI). This is consistent with the idea that the poor microtubule nucleating activity of the centrosome-related bodies is due to an abnormal protein set, distinguishing them from true centrosomes. Figure 6C, panel VI also shows an elongated nucleus-associated centrosome, which is consistent with the previously shown MTOC aberrations visualized by DdCP224 staining. Consistent with these defects being due to the knockout of DdCenB, only 4.2% of the DdCenB knockout cells expressing RFP-DdCenB (4 out of 94 cells) exhibited centrosome defects. Centrosome aberrations were rarely observed in AX3 cells (approximately 1%; 1 out of 98 cells).

Based on the effects of abrogation of DdCenB on the *D. discoideum* nucleus and centrosome, we searched for potential defects at the nucleus-centrosome connection by examining the localization of DdSun1 in DdCenB knockout cells. Using DdSun1 as a marker for the NE, we found that 91.2% of the

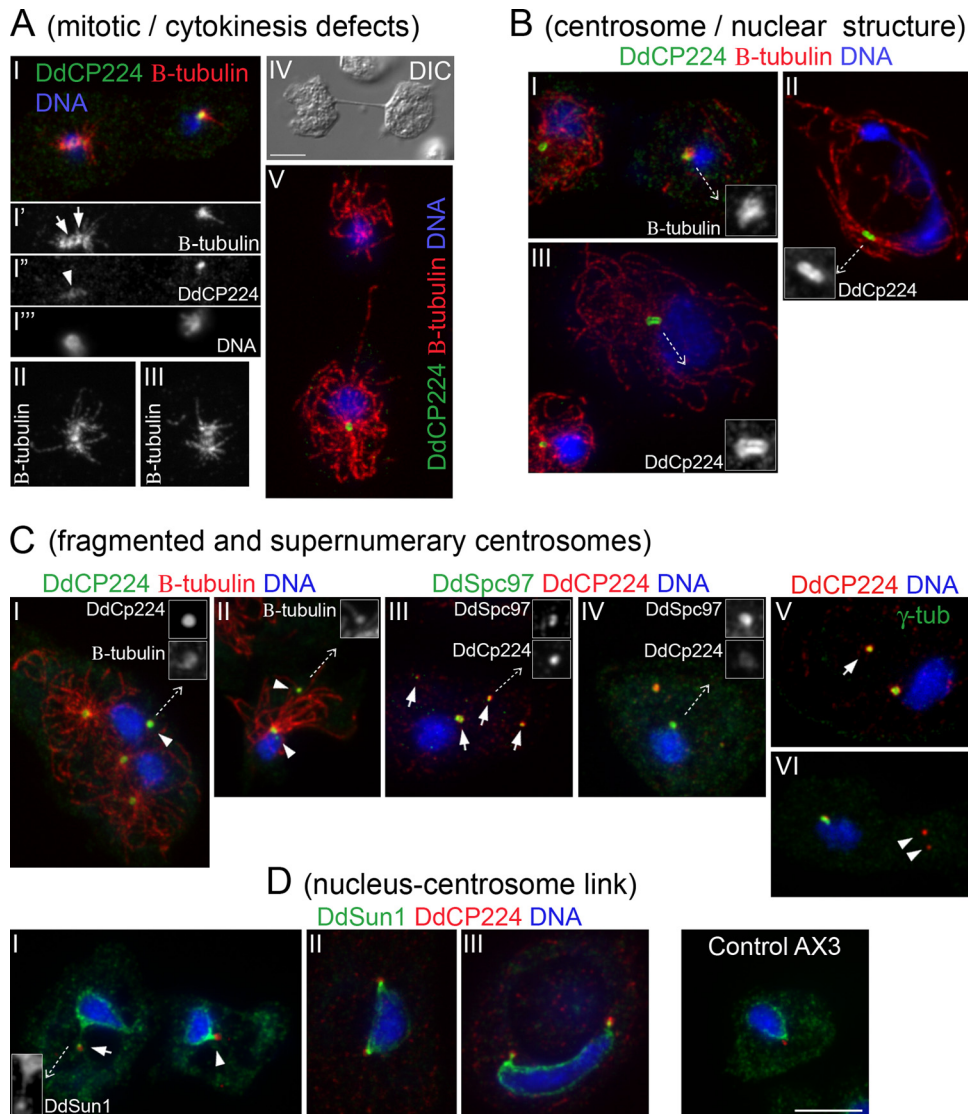


FIG. 6. Loss of DdCenB results in multiple defects at the nucleus and centrosome. The different phenotypes were assembled into four different groups based on similarity (as shown in the figure). All confocal images are brightest point projections of z-stacks consisting of 11 slices of 0.2 μm each. Insets show 3 \times magnification of confocal images. Cells were fixed with cold methanol and immunostained as indicated. DdCP224 (A, B, panels I and II of C), DdSpc97, γ -tubulin, and DdSun1 were visualized by immunostaining with rabbit antibodies. Anti-DdCP224 (panels III to VI of C, D) and anti- β -tubulin were mouse monoclonal antibodies. Secondary antibodies were anti-mouse Alexa 568 and anti-rabbit Alexa 488. DNA was stained with DAPI. The arrows in I' of panel A point to microtubule nucleation sites along the mitotic spindle. The arrowhead in panel I' of panel A points to diffusely localized DdCP224 along the spindle microtubules. The arrowhead in I of panel C and the arrowheads in II of panel C point to centrosome-related bodies of various sizes, morphologies, and microtubule nucleating abilities. The arrows in III of panel C point to the colocalization of DdCP224 and DdSpc97 at centrosomes and centrosome-related bodies. The arrow and arrowheads in V and VI of panel C point to the colocalization of DdCP224 and γ -tubulin at centrosome-related bodies. The arrow in I of panel D points to a long NE protrusion. The arrowhead in I of panel D points to a short NE protrusion. Bars, 5 μm . DIC, differential interference contrast.

cells lacking DdCenB had protrusions of the NE (92 out of 101 cells). Most of these protrusions were short in length, but some reached over half a nuclear diameter (Fig. 6D, panel I). We were also able to distinguish two types of NE protrusions; the most common type (65.1%) was hairpin shaped with a bulky head that was connected to the centrosome. The second type was shorter and appeared thicker due to the high concentration of DdSun1. Sixty-nine percent of DdCenB knockout cells expressing RFP-DdCenB (78 out of 109 cells) and 84% of AX3 cells (16 out of 100 cells) did not exhibit nuclear protrusions,

and the centrosomes were located proximal to the nuclei (as shown in the Control AX3 panel of Fig. 6D). Visualization of the NE by DdSun1 staining also showed that some interphase cells with supernumerary centrosomes had more than one MTOC attached to the nucleus. Figure 6D, panel II shows a cell with two centrosomes attached at almost opposite ends of the nucleus, thus pulling in different directions and causing the large nucleus to become elongated. This may also explain the presence of "dumbbell"-shaped nuclei (Fig. 6B, panel II), responding to torsional forces generated by two MTOCs rotating

in opposite directions. The nucleus-centrosome link in some of these cells was also altered by the lack of DdCenB, showing the same NE protrusions observed in cells containing a single centrosome (Fig. 6D, panel III). Taken together, the above results indicate that DdCenB is required to maintain proper centrosome/nuclear architecture.

DISCUSSION

Structural and phylogenetic analysis. DdCenB is a bona fide centrin with several unique features. The DdCenB N-terminal extension (also called the N-terminal subdomain) is relatively long and very close to the 23-amino-acid extensions typical of centrins (12), thus distinguishing DdCenB from the calmodulins. This extension has been suggested to confer upon centrins their functional diversity, and for at least one member of the centrin family, this extension has been shown to mediate calcium-dependent polymerization (51). At the C terminus, DdCenB retains the positively charged duplet (KK) and the 3-amino-acid extension beyond the fourth EF-hand domain characteristic of the centrin 1/2 group. Although the significance of this is unclear, this end of the protein is known to play a role in human centriolar duplication (34) and to mediate protein-protein interactions. For example, in the flagellated green algae *C. reinhardtii*, the terminal SLF¹⁶⁹ residues interact with the centrin binding domain of Kar1 (22); and when in complex, the S¹⁶⁷ is inaccessible for phosphorylation (35). Similarly, the hydrophobic residues at the C-terminal end of DdCenB might be responsible for protein-protein interactions, although there is no known homolog of Kar1 in *D. discoideum*. These interacting proteins could account for the functionality as well as the proper localization of DdCenB.

Phylogenetic analysis groups DdCenB with DdCenA in a divergent and monophyletic clade distinct from the spasmins and calmodulins. Furthermore, when DdCenB is compared to the consensus sequence of all the centrins included in the analysis, it shares identity with 17 out of the 19 (89%) fully conserved residues found across all of the centrins examined. This contrasts with the low level of identity shared with the conserved residues of calmodulins (17%) and spasmins (18%). The high level of divergence of DdCenB from other centrins is not a particular characteristic of this centrin protein but is common to many *D. discoideum* proteins. For example, DdCenA shares only 33 to 35% homology and 55 to 56% similarity to human centrins and was originally described as a centrin-related protein because it was the most divergent member reported to date (5). Likewise, DdCalB was suggested only to be related to calmodulins, due to its low sequence identity with other calmodulins (44). This level of divergence reflects the evolutionary history of the Dictyosteliidae, which constitute a monophyletic group that branched off the eukaryotic lineage after plants and before fungi and animals. Taken together, the structural features and the phylogenetic analysis indicate that DdCenB is a bona fide member of the centrin family.

DdCenB localization. The name “centrin” refers to the typical localization to the centriole (and related basal body). However, centrin localization is typically not confined to the MTOCs, even in cell types with prominent centriolar localization. In human cells, for example, it has been estimated that

only 10% of centrins localize to the centrioles (12, 40). In many acentriolar organisms, centrins are prominent in the nucleus. Such is the case for many plants (6) and budding and fission yeasts (39, 49). Interestingly, *D. discoideum* DdCenA is found at the nucleus in addition to the centrosome (5). Hence, the nuclear localization of DdCenB is peculiar but not unprecedented. The fact that both RFP-DdCenB and FLAG-DdCenB show identical localization patterns, while not generating any obvious phenotype, supports our argument that they reflect the localization of endogenous DdCenB. In addition, RFP-tagged DdCenB rescued the DdCenB knockout cell line from abnormal multinucleation levels (Fig. 5) and centrosome and nuclear defects. This suggests that RFP-DdCenB is functionally active and is concordant with previous reports on functionally active N-terminal GFP fusions of centrins in other organisms (2, 27, 54, 60).

One interesting aspect of the nuclear localization of DdCenB is the fact that this is lost as cells progress through mitosis until the completion of cytokinesis (Fig. 4A). The depletion of a centrin protein from a target organelle is very atypical, shared only by the other *D. discoideum* centrin, DdCenA (which is lost from the centrosome during mitosis) (5), and some plant centrins. However, centrosomal delocalization of DdCenA is not unexpected since its predominant centrosomal localization is at the corona, which is disassembled during centrosomal division. Del Vecchio et al. showed that in several mono- and dicotyledonous plants, centrin changed from cytoplasmic and nuclear locations in interphase cells to the mitotic matrix and cell plate in dividing cells (6). However, seed plant cells do not have discrete MTOCs comparable to animal centrosomes, and the NE serves as the main site of microtubule assembly (50). It could be argued that the disappearance of DdCenB from the NE at mitosis is due to the structural changes that the NE undergoes to allow for the ingression of the mitotic spindle, leading to fenestrations in the membrane and the diffusion of RFP-DdCenB out of the nucleus. However, the dynamic localization of RFP-DdCenB throughout mitosis is very different from the proposed passive diffusion out of the nucleus observed when GFP is fused to a nuclear localization signal (NLS) (59). Zhang and coworkers showed that the NLS-GFP begins disappearing from the *D. discoideum* nucleus at early mitosis until anaphase and returns at telophase. However, some level of NLS-GFP is retained in the nucleus at all stages (59). Further support against delocalization of DdCenB by simple diffusion is obtained by comparing its dynamic localization with that of DdHcpA and DdHcpB. The *D. discoideum* heterochromatin proteins HcpA and HcpB are similar in size to DdCenB (26 and 27 kDa, respectively, compared to 17 kDa) and experience nuclear delocalization at mitosis by a proposed diffusion mechanism (24). Again, the delocalization of these proteins from the nucleus is only partial and limited to a period between early mitosis and late anaphase. In contrast, RFP-DdCenB is lost from the nucleus at early mitosis and does not return until the completion of cytokinesis. All of the above, and the presence of DdCenB in the nuclei of cells dividing by traction-mediated cytofission (Fig. 4F), suggest that the dynamic localization of DdCenB is indeed actively regulated in a cell cycle-dependent manner. At this point we cannot discard

the possibility that the loss of DdCenB from the nucleus at mitosis is due to protein degradation.

Nuclear phenotypes associated with DdCenB knockout. As described above, few roles for centrins at the nucleus have been elucidated. These roles were largely unexpected for proteins that were originally associated with MTOC function. DdCenB presents a special case among centrins, since its primary localization is at the NE and is not limited to a specialized region as is CDC31 in yeast. Deletion of DdCenB led to multiple nuclear defects, including enlarged and elongated nuclei (Fig. 6B, panels II and III). These enlarged nuclei could arise from either nuclear fusion or karyokinesis defects during cell division. Although these are not mutually exclusive, we currently favor the idea that the genesis of these large nuclei is through defects in karyokinesis. Since the NE does not break down during mitosis in this organism, the failure to disassemble the mitotic spindle (as shown in Fig. 6A, panel V) could lead to the formation of a single, enlarged nucleus in the cell. One consistent characteristic of cells with enlarged nuclei was that they also had either two, normal-sized centrosomes or a single enlarged centrosome. These enlarged centrosomes may form from the fusion of nucleus-attached supernumerary MTOCs, a phenomenon that has been previously documented in *D. discoideum* for cytoplasmic supernumerary MTOCs (18).

In addition to the enlarged nuclei in DdCenB knockout cells, over 90% of these cells had NE protrusions that extended toward the centrosome, reminiscent of those observed upon expression of mutant DdSun1 (58). DdSun1 in the NE has been shown to interact with chromatin and thereby provides a firmer anchor to the centrosome. The observed NE protrusions in the DdCenB knockout cells suggest that DdCenB contributes to the anchoring of the nucleus-centrosome link to chromatin, potentially acting as an accessory protein that strengthens this anchoring. Consistent with this is the observed accumulation of DdSun1 at these protrusions in DdCenB knockout cells, possibly to increase potential sites of interaction with chromatin.

Centrosome phenotypes associated with DdCenB knockout. Loss of connection between the centrosome and the nucleus has previously been reported as a basis for centrosome hyperamplification (58). However, DdCenB knockdown cells also exhibited other centrosome defects, including the formation of centrosome-related bodies, centrosomes with poor microtubule nucleation, and enlarged centrosomes (discussed above), all suggesting that the functional roles of DdCenB extend beyond the anchoring of the centrosome. The profound effects that abrogation of DdCenB had on the centrosome (even though it predominantly localizes to the nucleus) could be explained by the atypical centrosome cycle of *D. discoideum*. As described above, duplication of the centrosome involves the transition of the dividing MTOC in and out of the NE (see the introduction). These transitions resemble the insertion of the SPB duplication plaque into the NE in budding yeast, suggesting that some of the structural and regulatory machinery might be conserved between *D. discoideum* and yeast. Centrosome duplication in *D. discoideum* is not synchronized with DNA synthesis, as in higher eukaryote MTOCs or budding yeast, but rather starts at the G₂/M transition (52). The beginning of centrosome division involves disassembly of the corona and fibrous link to the nucleus, followed by inser-

tion at the NE during prometaphase. This process includes the relocation of some of the corona components to the mitotic nuclear-embedded centrosome core. One dynamic component of the corona is DdCP224, a true centrosome protein that has been visualized in microtubule-free isolated centrosomes (16). DdCenB knockout cells had diffuse staining of DdCP224 at the mitotic poles (Fig. 6A), suggesting that the loss of DdCenB results in the abnormal transition of DdCP224 (and maybe other corona components) between the corona and the dividing nuclear-embedded centrosome. Subsequently, this aberrant localization of DdCP224 could have persisted in some centrosomes during interphase, resulting in poor microtubule nucleation (Fig. 6B, panel I). Furthermore, the abnormal transition may have caused most of the DdCP224 to relocate from the true MTOC to the centrosome-related bodies in the cytoplasm (Fig. 6C). Despite changes in DdCP224 localization, DdSpc97 and γ -tubulin were always observed at mitotic poles and nuclei-associated MTOCs (Fig. 6C). This suggests that the nucleus-associated centrosomes retained some level of protein organization at the corona. Differently, the protein composition of cytoplasmic centrosome-related bodies differed in the presence and abundance of both DdSpc97 and γ -tubulin. This is consistent with the inability of most of these bodies to nucleate microtubules, and suggests that, although they contain some MTOC proteins, most are not complete centrosomes.

Based on all of the above data, we suggest that the functional role of DdCenB is linked to the centrosome cycle and is defined by its dynamic localization. During interphase, DdCenB is at the nucleus and is involved in nuclear architecture and centrosome anchoring to the nucleus. We propose that before disappearing from the nucleus, DdCenB is part of the machinery that allows for proper centrosome cycle dynamics, including insertion in the NE (as proposed in budding yeast), and corona-related protein reorganization. Loss of DdCenB would lead to abnormal centrosome ingression in the NE and poor regulation of centrosome division, generating supernumerary centrosomes and centrosome-related bodies.

DdCenB has retained the cell cycle-regulated localization that so far has been observed only in plant centrins. This, and the evolutionary history of both lineages, suggests that the nuclear localization was one of the ancestral centrin features of early eukaryotes. Although centrins have been linked to diverse cellular activities, their most common and widely spread cellular function is related to MTOCs. DdCenB is no exception, which is significant since *D. discoideum* centrosomes share some structural characteristics with yeast, while at the same time its corona of amorphous material and its semiconservative replication are more reminiscent of higher eukaryote MTOCs. Consequently, *D. discoideum* may serve as an important bridge organism with which to expand our understanding of the evolution and function of these ubiquitous proteins.

ACKNOWLEDGMENTS

We appreciate the generosity of Stephen Doxsey for allowing us access to his confocal microscope and to Samba Redick for assisting us in its use. We also appreciate the help of Camilo Khatchikian and Jason Slot with the phylogenetic analysis. We thank Richard Sugang for providing us with the REMI construct that allowed us to generate the knockout cell line. Finally, we are thankful of Clement Nizak, Annette Muller-Taubenberger, and the *D. discoideum* Stock Center for the development and distribution of pTX-mRFPmars.

This work was supported, in part, through a Faculty Development Award from Clark University to D.A.L.

REFERENCES

- Chen, L., and K. Madura. 2008. Centrin/Cdc31 is a novel regulator of protein degradation. *Mol. Cell. Biol.* **28**:1829–1840.
- D'Assoro, A. B., F. Stivala, S. Barrett, G. Ferrigno, and J. L. Salisbury. 2001. GFP-centrin as a marker for centriole dynamics in the human breast cancer cell line MCF-7. *Ital. J. Anat. Embryol.* **106**:103–110.
- Dauderer, C., and R. O. Graf. 2002. Molecular analysis of the cytosolic Dictyostelium gamma-tubulin complex. *Eur. J. Cell Biol.* **81**:175–184.
- Dauderer, C., M. Schliwa, and R. Graf. 1999. *Dictyostelium discoideum*: a promising centrosome model system. *Biol. Cell* **91**:313–320.
- Dauderer, C., M. Schliwa, and R. Graf. 2001. *Dictyostelium* centrin-related protein (DdCp), the most divergent member of the centrin family, possesses only two EF hands and dissociates from the centrosome during mitosis. *Eur. J. Cell Biol.* **80**:621–630.
- Del Vecchio, A. J., J. D. I. Harper, K. C. Vaughn, A. T. Baron, J. L. Salisbury, and R. L. Overall. 1997. Centrin homologues in higher plants are prominently associated with the developing cell plate. *Protoplasma* **196**:224–234.
- Dinh, C., J. Ong, J. Martinez, V. Korchina, J. Fraser, N. Mai, T. Luong, V.-T. Dinh, J. Hu, J. Song, R. Sugang, G. Shaulsky, and A. Kuspa. 2006. A strategy to generate 23,000 individual barcoded *D. discoideum* insertion mutants for the parallel analysis of phenotypes, abstr. 121. International Dictyostelium Conference, Santa Fe, NM, 17 to 22 September 2006.
- Eichinger, L., J. A. Pachebat, G. Glockner, M. A. Rajandream, R. Sugang, M. Berriman, J. Song, R. Olsen, K. Szafrański, Q. Xu, B. Tungal, S. Kummerfeld, M. Madera, B. A. Konfortov, F. Rivero, A. T. Kohler, R. Lehmann, N. Hamlin, R. Davies, P. Gaudet, P. Fey, K. Pilcher, G. Chen, D. Saunders, E. Sodergren, P. Davis, A. Kerhornou, X. Nie, N. Hall, C. Anjard, L. Hemphill, N. Bason, P. Farbrother, B. Desany, E. Just, T. Morio, R. Rost, C. Churcher, J. Cooper, S. Haydock, N. van Driessche, A. Cronin, I. Goodhead, D. Muzny, T. Mourier, A. Pain, M. Lu, D. Harper, R. Lindsay, H. Hauser, K. James, M. Quiles, M. Madan Babu, T. Saito, C. Buchrieser, A. Wardroper, M. Felder, M. Thangavelu, D. Johnson, A. Knights, H. Louseged, K. Mungall, K. Oliver, C. Price, M. A. Quail, H. Urushihara, J. Hernandez, E. Rabinowitsch, D. Steffen, M. Sanders, J. Ma, Y. Kohara, S. Sharp, M. Simmonds, S. Spiegler, A. Tivey, S. Sugano, B. White, D. Walker, J. Woodward, T. Winckler, Y. Tanaka, G. Shaulsky, M. Schleicher, G. Weinstock, A. Rosenthal, E. C. Cox, R. L. Chisholm, R. Gibbs, W. F. Loomis, M. Platzer, R. R. Kay, J. Williams, P. H. Dear, A. A. Noegel, B. Barrell, and A. Kuspa. 2005. The genome of the social amoeba *Dictyostelium discoideum*. *Nature* **435**:43–57.
- Errabolu, R., M. A. Sanders, and J. L. Salisbury. 1994. Cloning of a cDNA encoding human centrin, an EF-hand protein of centrosomes and mitotic spindle poles. *J. Cell Sci.* **107**:9–16.
- Euteneuer, U., R. Graf, E. Kube-Grandenrath, and M. Schliwa. 1998. Dictyostelium gamma-tubulin: molecular characterization and ultrastructural localization. *J. Cell Sci.* **111**:405–412.
- Fischer, T., S. Rodriguez-Navarro, G. Pereira, A. Racz, E. Schiebel, and E. Hurt. 2004. Yeast centrin Cdc31 is linked to the nuclear mRNA export machinery. *Nature Cell Biol.* **6**:840–848.
- Friedberg, F. 2006. Centrin isoforms in mammals. Relation to calmodulin. *Mol. Biol. Rep.* **33**:243–252.
- Gavet, O., C. Alvarez, P. Gaspar, and M. Bornens. 2003. Centrin4p, a novel mammalian centrin specifically expressed in ciliated cells. *Mol. Biol. Cell* **14**:1818–1834.
- Graf, R. 2001. Isolation of centrosomes from Dictyostelium. *Methods Cell Biol.* **67**:337–357.
- Graf, R., C. Dauderer, and M. Schliwa. 1999. Cell cycle-dependent localization of monoclonal antibodies raised against isolated Dictyostelium centrosomes. *Biol. Cell* **91**:471–477.
- Graf, R., C. Dauderer, and M. Schliwa. 2000. Dictyostelium DdCP224 is a microtubule-associated protein and a permanent centrosomal resident involved in centrosome duplication. *J. Cell Sci.* **113**:1747–1758.
- Graf, R., C. Dauderer, and I. Schulz. 2004. Molecular and functional analysis of the Dictyostelium centrosome, p. 155–202. International review of cytology, vol. 241. Elsevier Academic Press, San Diego, CA.
- Graf, R., U. Euteneuer, T. H. Ho, and M. Rehberg. 2003. Regulated expression of the centrosomal protein DdCP224 affects microtubule dynamics and reveals mechanisms for the control of supernumerary centrosome number. *Mol. Biol. Cell* **14**:4067–4074.
- Guerin, N. A., and D. A. Larochelle. 2002. A user's guide to restriction enzyme-mediated integration in Dictyostelium. *J. Muscle Res. Cell Motil.* **23**:597–604.
- Hall, T. A. 1999. BioEdit: a user-friendly biological sequence alignment editor and analysis program for Windows 95/98/NT. *Nucleic Acids Symp. Ser.* **41**:95–98.
- Hartman, H., and A. Fedorov. 2002. The origin of the eukaryotic cell: a genomic investigation. *Proc. Natl. Acad. Sci. USA* **99**:1420–1425.
- Hu, H., and W. J. Chazin. 2003. Unique features in the C-terminal domain provide caltractin with target specificity. *J. Mol. Biol.* **330**:473–484.
- Ivanovska, I., and M. D. Rose. 2001. Fine structure analysis of the yeast centrin, Cdc31p, identifies residues specific for cell morphology and spindle pole body duplication. *Genetics* **157**:503–518.
- Kaller, M., U. Euteneuer, and W. Nellen. 2006. Differential effects of heterochromatin protein 1 isoforms on mitotic chromosome distribution and growth in *Dictyostelium discoideum*. *Eukaryot. Cell* **5**:530–543.
- Katz, E. R. 2006. Kenneth Raper, Elisha Mitchell and *Dictyostelium*. *J. Biosci.* **31**:195–200.
- Koblentz, B., J. Schoppmeier, A. Grunow, and K. F. Lechtreck. 2003. Centrin deficiency in *Chlamydomonas* causes defects in basal body replication, segregation and maturation. *J. Cell Sci.* **116**:2635–2646.
- Kuriyama, R., Y. Terada, K. S. Lee, and C. L. Wang. 2007. Centrosome replication in hydroxyurea-arrested CHO cells expressing GFP-tagged centrin2. *J. Cell Sci.* **120**:2444–2453.
- Kuspa, A., and W. F. Loomis. 1994. REMI-RFLP mapping in the Dictyostelium genome. *Genetics* **138**:665–674.
- Laoukili, J., E. Perret, S. Middendorp, O. Houcine, C. Guennou, F. Marano, M. Bornens, and F. Tournier. 2000. Differential expression and cellular distribution of centrin isoforms during human ciliated cell differentiation in vitro. *J. Cell Sci.* **113**:1355–1364.
- LeDizet, M., and G. Piperno. 1995. The light chain p28 associates with a subset of inner dynein arm heavy chains in *Chlamydomonas* axonemes. *Mol. Biol. Cell* **6**:697–711.
- Lee, V. D., and B. Huang. 1993. Molecular cloning and centrosomal localization of human caltractin. *Proc. Natl. Acad. Sci. USA* **90**:11039–11043.
- Levi, S., M. Polyakov, and T. T. Egelhoff. 2000. Green fluorescent protein and epitope tag fusion vectors for Dictyostelium discoideum. *Plasmid* **44**:231–238.
- Levy, Y. Y., E. Y. Lai, S. P. Remillard, M. B. Heintzelman, and C. Fulton. 1996. Centrin is a conserved protein that forms diverse associations with centrioles and MTOCs in *Naegleria* and other organisms. *Cell Motil. Cytoskeleton* **33**:298–323.
- Lutz, W., W. L. Lingle, D. McCormick, T. M. Greenwood, and J. L. Salisbury. 2001. Phosphorylation of centrin during the cell cycle and its role in centriole separation preceding centrosome duplication. *J. Biol. Chem.* **276**:20774–20780.
- Meyn, S. M., C. Seda, M. Campbell, K. L. Weiss, H. Hu, B. Pastrana-Rios, and W. J. Chazin. 2006. The biochemical effect of Ser167 phosphorylation on *Chlamydomonas reinhardtii* centrin. *Biochem. Biophys. Res. Commun.* **342**:342–348.
- Middendorp, S., A. Paoletti, E. Schiebel, and M. Bornens. 1997. Identification of a new mammalian centrin gene, more closely related to *Saccharomyces cerevisiae* CDC31 gene. *Proc. Natl. Acad. Sci.* **94**:9141–9146.
- Moncrief, N. D., R. H. Kretsinger, and M. Goodman. 1990. Evolution of EF-hand calcium-modulated proteins. I. Relationships based on amino acid sequences. *J. Mol. Evol.* **30**:522–562.
- Nishi, R., Y. Okuda, E. Watanabe, T. Mori, S. Iwai, C. Masutani, K. Sugawara, and F. Hanaoka. 2005. Centrin 2 stimulates nucleotide excision repair by interacting with xeroderma pigmentosum group C protein. *Mol. Cell Biol.* **25**:5664–5674.
- Paoletti, A., N. Bordes, R. Haddad, C. L. Schwartz, F. Chang, and M. Bornens. 2003. Fission yeast cdc31p is a component of the half-bridge and controls SPB duplication. *Mol. Biol. Cell* **14**:2793–2808.
- Paoletti, A., M. Moudjou, M. Painttrand, J. L. Salisbury, and M. Bornens. 1996. Most of centrin in animal cells is not centrosome-associated and centrosomal centrin is confined to the distal lumen of centrioles. *J. Cell Sci.* **109**:3089–3102.
- Rasband, W. S. 1997–2008. ImageJ. National Institutes of Health, Bethesda, MD. <http://rsb.info.nih.gov/ij/>.
- Rehberg, M., and R. Graf. 2002. Dictyostelium EBI is a genuine centrosomal component required for proper spindle formation. *Mol. Biol. Cell* **13**:2301–2310.
- Ronquist, F., and J. P. Huelsenbeck. 2003. MrBayes 3: Bayesian phylogenetic inference under mixed models. *Bioinformatics* **19**:1572–1574.
- Rosel, D., F. Puta, A. Blahuskova, P. Smykal, and P. Folk. 2000. Molecular characterization of a calmodulin-like Dictyostelium protein CalB. *FEBS Lett.* **473**:323–327.
- Salisbury, J. L., A. Baron, B. Surek, and M. Melkonian. 1984. Striated flagellar roots: isolation and partial characterization of a calcium-modulated contractile organelle. *J. Cell Biol.* **99**:962–970.
- Salisbury, J. L., K. M. Suino, R. Busby, and M. Springett. 2002. Centrin-2 is required for centriole duplication in mammalian cells. *Curr. Biol.* **12**:1287–1292.
- Sanders, M. A., and J. L. Salisbury. 1994. Centrin plays an essential role in microtubule severing during flagellar excision in *Chlamydomonas reinhardtii*. *J. Cell Biol.* **124**:795–805.
- Schiebel, E., and M. Bornens. 1995. In search of a function for centrins. *Trends Cell Biol.* **5**:197–201.
- Spang, A., I. Courtney, U. Fackler, M. Matzner, and E. Schiebel. 1993. The calcium-binding protein cell division cycle 31 of *Saccharomyces cerevisiae* is

- a component of the half bridge of the spindle pole body. *J. Cell Biol.* **123**:405–416.
50. **Stoppin, V., M. Vantard, A. C. Schmit, and A. M. Lambert.** 1994. Isolated plant nuclei nucleate microtubule assembly: the nuclear surface in higher plants has centrosome-like activity. *Plant Cell* **6**:1099–1106.
51. **Tourbez, M., C. Firanesco, A. Yang, L. Unipan, P. Duchambon, Y. Blouquit, and C. T. Craescu.** 2004. Calcium-dependent self-assembly of human centrin 2. *J. Biol. Chem.* **279**:47672–47680.
52. **Ueda, M., M. Schliwa, and U. Euteneuer.** 1999. Unusual centrosome cycle in *Dictyostelium*: correlation of dynamic behavior and structural changes. *Mol. Biol. Cell* **10**:151–160.
53. **Uyeda, T. Q., A. Nagasaki, and S. Yumura.** 2004. Multiple parallelisms in animal cytokinesis. *Int. Rev. Cytol.* **240**:377–432.
54. **White, R. A., Z. Pan, and J. L. Salisbury.** 2000. GFP-centrin as a marker for centriole dynamics in living cells. *J. Electron Microsc. Tech.* **49**:451–457.
55. **Wiech, H., B. M. Geier, T. Paschke, A. Spang, K. Grein, J. Steinkotter, M. Melkonian, and E. Schiebel.** 1996. Characterization of green alga, yeast, and human centrins. Specific subdomain features determine functional diversity. *J. Biol. Chem.* **271**:22453–22461.
56. **Wolfrum, U., and J. L. Salisbury.** 1998. Expression of centrin isoforms in the mammalian retina. *Exp. Cell Res.* **242**:10–17.
57. **Wright, R. L., J. Salisbury, and J. W. Jarvik.** 1985. A nucleus-basal body connector in *Chlamydomonas reinhardtii* that may function in basal body localization or segregation. *Mol. Biol. Cell* **101**:1903–1912.
58. **Xiong, H., F. Rivero, U. Euteneuer, S. Mondal, S. Mana-Capelli, D. Laroche, A. Vogel, B. Gassen, and A. A. Noegel.** 2008. Dictyostelium Sun-1 connects the centrosome to chromatin and ensures genome stability. *Traffic* **9**:708–724.
59. **Zang, J.-H., G. Cavet, J. H. Sabry, P. Wagner, S. L. Moores, and J. A. Spudich.** 1997. On the role of myosin-II in cytokinesis: division of Dictyostelium cells under adhesive and nonadhesive conditions. *Mol. Biol. Cell* **8**:2617–2629.
60. **Zhong, Z., L. Spate, Y. Hao, R. Li, L. Lai, M. Katayama, Q. Sun, R. Prather, and H. Schatten.** 2007. Remodeling of centrosomes in intraspecies and interspecies nuclear transfer porcine embryos. *Cell Cycle* **6**:1510–1520.